

## Simultaneous Temperature and Velocity Fields Measurements near the Boiling Point

Deog-Hee Doh<sup>†</sup> · Tae-Gyu Hwang<sup>\*\*</sup> · Bon-Young Koo<sup>\*\*\*</sup> · Seok-Ro Kim<sup>\*\*\*</sup>

(Manuscript : Received JUN 26, 2007 ; Revised JUL 19, 2007)

**Abstract** : Simultaneous measurement technique for temperature and velocity fields near a heated solid body has been constructed. The measurement system consists of a 3-plate CCD color camera, a color image grabber, a lighting system, a host computer and a software for the whole quantification process. Thermo Chromic Liquid Crystals (TCLC) was used as temperature sensors. A neural network was used to get a calibration curve between the temperature and the color change of the TCLC in order to enhance the dynamic range of temperature measurement. The velocity field measurement was attained by the use of the gray-level images taken for the flow field, and by introducing the cross-correlation technique. The temperature and the velocity fields of the forced and the natural convective flows near the surface of a cartridge heater were measured simultaneously with the constructed measurement system.

**Key words** : Simultaneous measurement, temperature and velocity fields, cartridge heater, natural and forced flows

### Nomenclature

B, R, G : color intensity(0~255)  
 $C_{fg}$  : correlation coefficient  
 $f_i, g_i$  : gray level (i=1, 2, ..., 8, 9)  
H : Hue value  
 $S^*$  : variation of brightness  
 $t_k$  : teaching value of the neural network  
T : temperature [°C]  
 $T'$  : fluctuating temperature [°C]  
u : velocity [m/sec]

$u'$  : fluctuating velocity [m/sec]  
 $x_i$  : brightness of image(gray level)(i=1, 2, 3...)  
 $\bar{x}$  : mean value of brightness  
 $\delta$  : deviation from mean value(j=1, 2, 3...)

Simultaneous information on temperature and velocity fields is very useful for understanding not only for the convective heat transfer mechanism but also for the

<sup>†</sup> Corresponding Author(Korea Maritime Univ., Div. of Mech. & Info. Eng.), E-mail: doh@hhu.ac.kr, Tel: 051)410-4364

<sup>\*\*</sup> Division of Mechanical and Information Eng., Korea Maritime University

<sup>\*\*\*</sup> Dept. of Mech. Eng., Georgia Institute of Tech., U.S.A.

<sup>\*\*\*</sup> Dept. II, Refrigeration Div., Digital Appliance Co., LG Electronics

structure of the flow field itself because the local heat transfer coefficient can be calculated.

based upon the analogy between momentum and heat transfer.

Various temperature-measuring devices, such as mercury thermometers, thermocouples, resistance thermometers, and infrared thermometers are not able to provide simultaneous information on temperature and velocity fields of a thermal flow, which is inevitable to quantify the turbulent heat flux.

Klein<sup>(1)</sup> was the first researcher who used thermo-sensitive liquid crystal for flow visualizations in wind-tunnel experiments. He applied an unencapsulated liquid crystal to his test model, and qualitatively studied the steady-state boundary-layer temperature distributions of the model. Lemberg<sup>(2)</sup> used the same technique to visualize the unsteady boundary-layer on a model surface. Since the color play of the liquid crystal is sensitive to shear stress, the above techniques did not allow for accurate qualitative or quantitative temperature measurements. However, McEldery<sup>(3)</sup> solved this problem by using encapsulated liquid crystals in an experimental technique similar to Klein's technique. Orden and Hendricks<sup>(4)</sup> further advanced this technique for surface analysis in water tunnels by using liquid crystals covered with a layer of acrylic polymer and polyurethane coating. This shielded the crystals from shear stresses and prevented chemical contamination of the crystals by the water. Rhee et al.<sup>(5),(6)</sup> expanded the use of encapsulated liquid crystals to the

investigation of temperature distribution of the flow field rather than on model surface. By mixing the encapsulated liquid crystals with the working fluid and illuminating a two-dimensional cross-section of the flow with a white sheet of light, Dabiri and Gharib<sup>(7)</sup> were able to study heated vortexing. Color photographs showed pathlines, flow structures, and temperature distributions.

In the mean time, efforts have been made to quantify the temperature field through the use of liquid crystals. Cooper et al.<sup>(8)</sup> used encapsulated liquid crystals to measure the variation of the Nusselt number on a circular cylinder placed in a crossflow of air. Wilcox, et al.<sup>(9)</sup> proposed a color photography technique by introducing (TLC technique: Thermochromic Liquid Crystal Technique). Akino, et al.<sup>(10),(11)</sup> performed calibration of the wavelength of the color against temperature using a monochrome CCD camera and interference filters. Instead of calibrating temperature against location in R, G, B color space, Dabiri and Gharib<sup>(7)</sup> proposed the use of H, S, I color space with hue as the single calibration variable. Thus, they showed that a usable relationship could be established between the hue and the temperature. The Hue-value calibration has been successfully adopted to the studies of thermal phenomena by Ozawa, et al.<sup>(12)</sup>, Nozaki, et al.<sup>(13)</sup>.

In TLC technique, a color-to-temperature calibration is necessary to obtain the temperature distribution. However, it is not so easy to obtain the exact calibration because the characteristic curve of temperature and color shows

very strong non-linearity. Kimura et. al.<sup>(14)</sup> and Hwang et. al.<sup>(15)</sup> adopted a neural network to solve this problem. The number of the neuron of the hidden layer of their neural network was only three.

All of the temperature field measurements were restricted to lower temperature ranging from 10°C to 50 °C. Chang & Doh<sup>(16)</sup> successfully carried out a simultaneous measurement for a thermal fluid flow using TLC. However, the temperature range was lower than 40°C. Up to best knowledge of the authors, there have been no research reports on the temperature field measurements over 80 °C in water thermal flows due to difficulties of color-to-temperature calibration.

In this study, measurements on higher temperature flow fields near the water boiling point under atmospheric condition have been successfully attained, and simultaneous measurements on the velocity fields have also been made.

## 2. Measurements of Thermal Flows around a Cartridge Heater

A cartridge heater was installed into a Poly-carbonated water bath (60mm x 60mm x 350mm) of which temperature maintained around 86 °C. Thermal flows around the cartridge heater in forced and natural condition were measured by the simultaneous measurement system. A cartridge heater was installed at 20mm height from the tip of the heater and the heat was controlled by the voltage of the controller. The measurement area was set near the boundary of the surface of the

cartridge heater. The measurement system consists of a 3-plate CCD color camera, a color image grabber, a lighting system, a host computer and a software for the whole quantification process. A white lighting system (30W) was used to illuminate the flow field

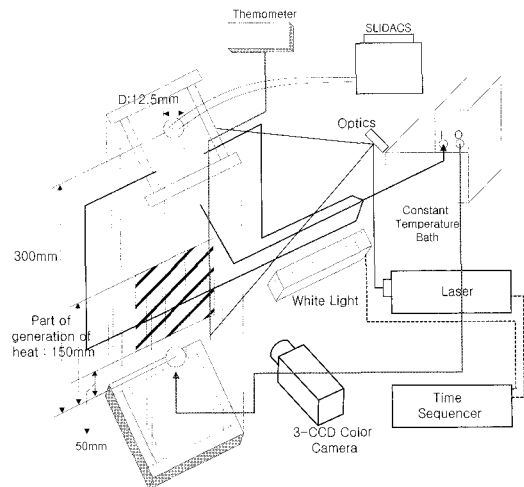


**Fig. 1 Simultaneous measurement system**

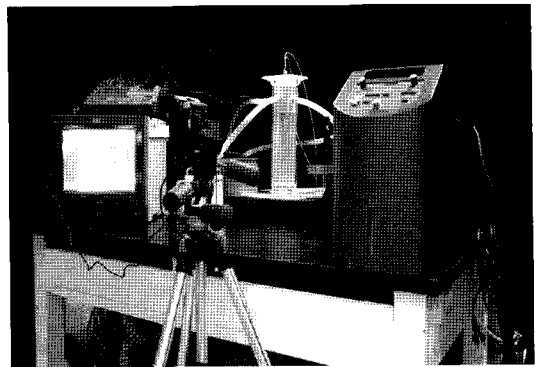


**Fig. 2 Picture of the system**

The angle between the illumination and the camera's viewing was set to about 40°. The color camera (713 x 512 pixels) was used for capturing the color change of the liquid crystals. Thermo Chromic Liquid Crystals (TCLC) was used as temperature

sensors. The colors of the liquid crystals vary with the temperature changes of the fluid between 86°C and 93.5°C. A color-to-temperature calibration was made in a stepwise manner. That is, the water of the basin was circulated by the constant temperature bath and each image of the flow field illuminated by the light was captured. The captured images were digitized into 8bit R, G, B color levels. The temperature of the circulating water was changed 0.5°C step for the color calibration. Calibration of color-to-temperature of the liquid crystal was carried out by changing the water temperature in stepwise with 0.5 °C. The temperature range of the calibration was 86°C to 93.5°C. After finishing the calibration, the cartridge heater was heated up to the temperature of showing colors, which means the temperature range of the flow was within the range of calibrated temperature. The temperature field in this quiescent state was measured. After this, a vertical jet was injected from the bottom of the water tank by opening a valve to make the flow field in forced condition. In forced flow condition the velocity field ranges from 0.05 m/s to 1.0 m/s.

Since the color variation of TCLC to the temperature change of the fluid shows very strong non-linearity, a neural network that is usually known as a non-linear fitting method has been used to expand the zone of linearity between the temperature and the color of TCLC<sup>[15]</sup>, which eventually enhances the dynamic range of temperature measurement.

The velocity field measurement was attained using the gray-level cross-correlation algorithm<sup>[17]</sup>. Detailed processing

for each quantification is mentioned in the next sections.

## 2.1 Temperature field measurements with a neural network algorithm

### 2.1.1 Color to temperature calibration

Fig. 3 shows the area that the color camera is viewing. The size of the actual measurement area is about 10 mm x 40 mm. Fig. 4 shows one of calibration images when the temperature in the water bath was uniformly maintained with 88°C. The uniformity was checked by measuring temperature at several points inside of the tank with a thermocouple.

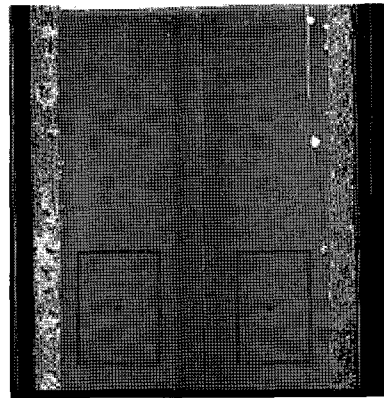


Fig. 3 Measurement region around the cartridge

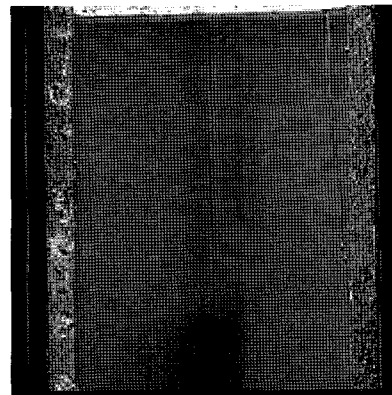


Fig. 4 Calibration image at 88°C

The color shows uniform distribution over the whole region since image capturing for the calibration was carried out when the water in the bath was circulated enough to make uniform temperature distribution for the whole area. Every image was captured with the image grabber (Ditect-64) through the 3-plate color camera at every calibration temperature. The images were separated into Red(R), Green(G) and Blue(B) images and their pixel colors is digitized into 256 gray levels, respectively. Since the quality of the image near the boundary of the heater surface was largely contaminated by the jittering effect of the image signal, which is usually seen at low intensity of lighting, a median filter as shown in Fig. 5 was used in order to enhance the quality of the image. The gray-level(intensity) value of the center pixel denoted as  $f_5$  is replaced with the values of the surrounded pixels. In order to reduce noises occurred by jitters, Thompson's Tau Method (1983) was used.

$$\bar{x} = \sum_{i=1}^N \frac{x_i}{N} \tag{1}$$

$$S^* = \sqrt{\sum_{i=1}^N \frac{(x_i - \bar{x})^2}{N}} \tag{2}$$

$$\delta = |x_j - \bar{x}| \tag{3}$$

f1	f2	f3
f4	f5	f6
f7	f8	f9

$$f_5 = \frac{f1 + f2 + f3 + f4 + f5 + f6 + f7 + f8 + f9}{9}$$

Fig. 5 Median filter

In this method, if  $(\delta \geq \tau \cdot S^*)$ , then  $x_j$  is eliminated. If  $(\delta \tau < \tau \cdot S^*)$ , then  $x_j$  is not eliminated during the process of the Median filtering. Here,  $x_j$  is the intensity of the colors of the pixels. Other letters represent as the below equations, such as the mean intensity and the standard deviation of the intensity. Generally, Hue (H) values have been used for quantifying the color information using R, G and B values. Eq. (4) is H value for color quantification.

$$H = \cos^{-1} \left\{ \frac{1/2[(R-G)+(R-B)]}{\left[ (R-G)^2 + (R-B)(G-B) \right]^{1/2}} \right\},$$

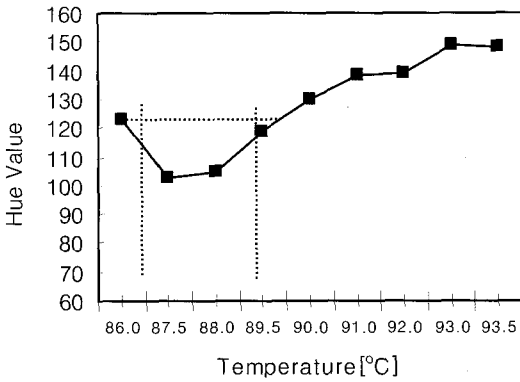
(at  $B \leq G$ )

$$H = 2\pi - \cos^{-1} \left\{ \frac{1/2[(R-G)+(R-B)]}{\left[ (R-G)^2 + (R-B)(G-B) \right]^{1/2}} \right\},$$

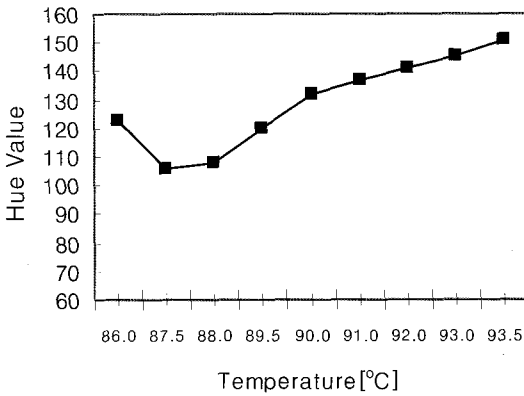
(at  $B > G$ )

(4)

Fig. 6(a) and (b) show the relations between the color and its corresponding temperature for the left and right measurement regions. Since the illuminating light conditions are not same, two calibration regions were considered. With the values of H, it is not so easy to define a function of color-to-temperature because two temperatures values exist for one Hue value as seen as dotted line in Fig. 6. It can be said that there are two temperatures values for one Hue value (dotted line in Fig. 6), which implies that the temperature measurements can't be attained at lower temperature region.



(a) For the left region shown on Fig. 3



(b) For the right region shown on Fig. 3

**Fig. 6 Relations between color and temperature**

In order to solve this problem, a neural network has been adopted. Neural network is well known for its strong capability of fitting any strong non-linear curves into linear function. Fig. 7 shows the used neural network. The network consists of three layers, input, hidden and output. The number of the hidden layer is 50. As the inputs of the neural network, the color information of R, G, B, and H were used. Here,  $\theta$  and  $\gamma$  are offset values for color noise. R, G, B and H values are used for training the neural network. The calculation algorithm is based on the back-propagation<sup>[18]</sup>. The

calculation is repeated until the Error value (E) between  $t_k$  and  $z_k$  becomes smaller than a threshold value.  $t_k$  is the temperature at which the color information (R, G, B, H) is used as the input of the neural network. The value  $t_k$  is usually called the teaching value of the neural network while  $z_k$  is expressed as Eq. (5).

$$t_k = f_x = \frac{1}{(1 + e^{-(ax + b)})} \quad (5)$$

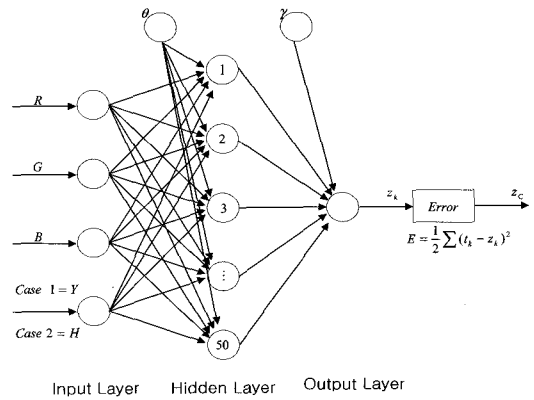


**Fig. 7 Used neural network**

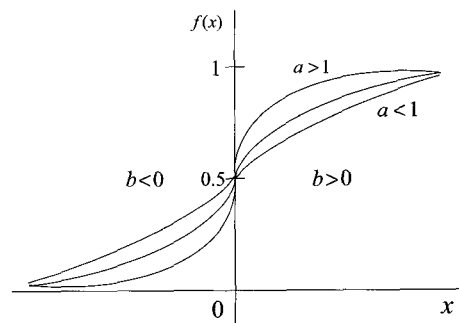


**Fig. 8 Used Sigmoid function**

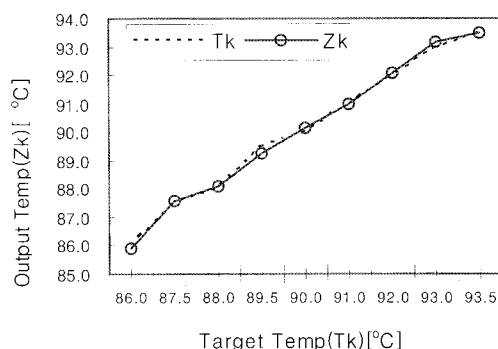
Here, a and b are integer obtained in the process of calculating the neural network<sup>[18]</sup>. The sigmoid function as shown on Fig. 8 was used as the output of every neuron. In the calculation

process of neural network, every weight is newly calculated using the back-propagation in which the outputs of every neuron were newly adjusted toward the smallest error value (E value). Ten learning patterns were taught to the neuron and the weights were decided when the error E was small enough than a threshold value.

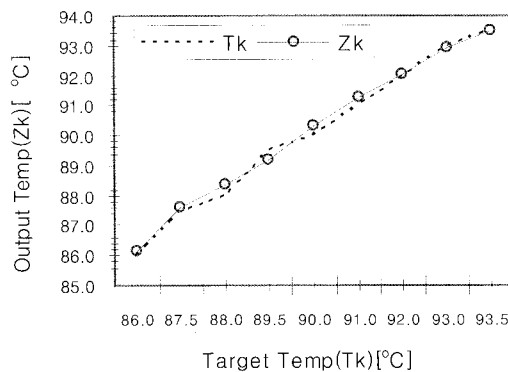
Fig. 9(a) and (b) show the calibration curves obtained by the neural network for the left and right regions of the cartridge heater(L:300mm, D:12.5mm, 800W). As shown on Fig. 6(a) and (b) the relation of temperature-to-color can be mapped by using this calibration curve when measuring temperature fields for both measurement regions. Tk means the teaching temperature and is measured by the thermocouples. The temperature values are trained at the output of the neural network while the corresponding color information, R, G, B and H are trained to the input. In this manner, the coefficients of the hidden layers of the neural network are adjusted nonlinearly for the whole input and output data sets. As mentioned previously, Zk means the temperature obtained at the output layer of the network.

Once the calibration is completed, this temperature is explicitly and directly obtained just by putting the color information (R, G, B and H) of every image pixels into the input layer of the network, which is the advantage of using the neural network. It can be seen that slight difference exists between the input and the output temperatures. The total relative error for the measured temperature range was about 5%, and it

was obtained by the standard statistical data process<sup>[19]</sup>. Once the neural network is taught, the output temperature is decided straightforwardly just by putting the color information, R, G, B and H values into the input layer. In order to reduce inhomogeneous light scattering effects, multi-sectional color information was used for constructing. The temperature measurement was carried out using the neural network having this capability.



(a) For the left region on Fig. 3



(b) For the right region on Fig. 3

**Fig. 9 Calibration results obtained by the neural network**

### 2.1.2 Measurements under steady and unsteady (forced jet) states

Fig. 10 shows one of instantaneous images under quiescent flow state while main-

taining the water temperature 86°C and making the cartridge heater heated by the use of the slide voltage controller. Putting the color information (R, G, B and H) onto the input layer of the neural network that had already been trained in the calibration process directly produces an output temperature at the output layer of the network. Fig. 11 shows one of

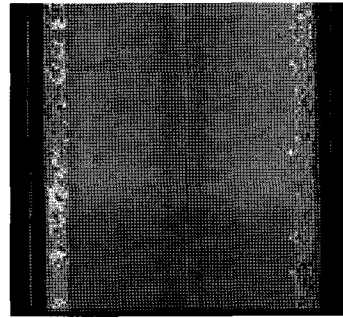
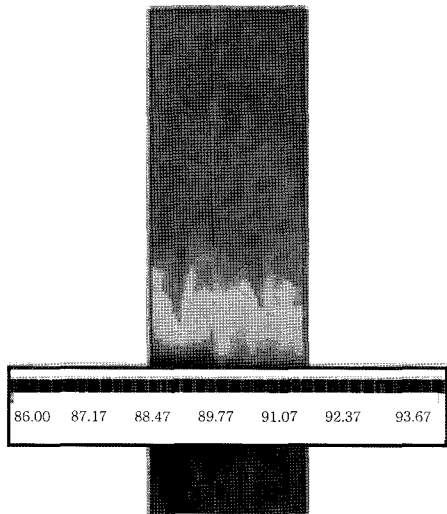
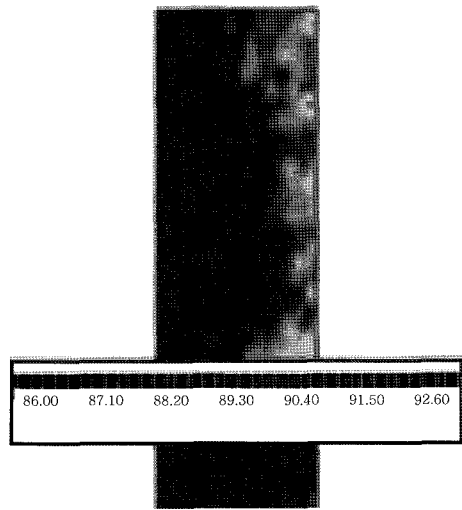


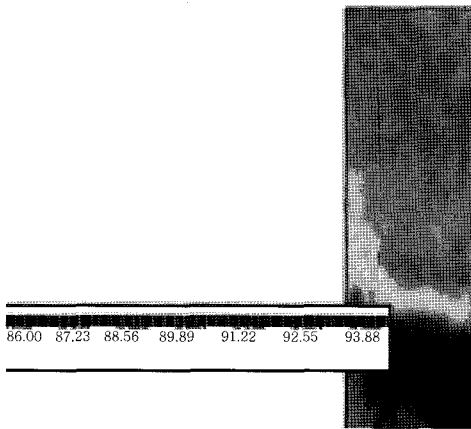
Fig. 10 Instantaneous color image



(a) Left region

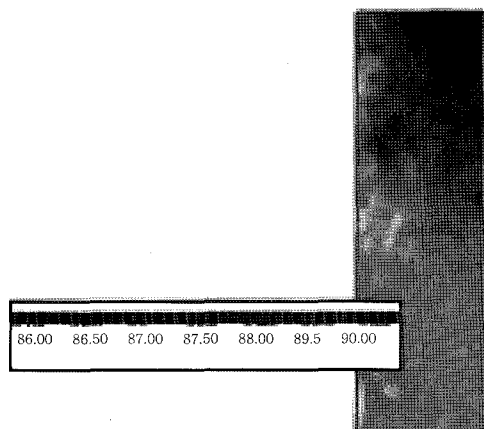


(a) Left region



(b) Right region

Fig. 11 Measured temperature field obtained by the neural network(quiescent state)



(b) Right region

Fig. 12 Measured temperature field obtained by the neural network(forced jet state)



the measured results calculated by the constructed neural network for the instantaneous image shown on Fig. 10. Fig. 11(a) shows the results obtained at the left region of the cartridge heater. The results show those obtained near the boundary of the heater and of which size is 10 mm x 40 mm. The quasi colors shown on Fig. 11(a) and (b) mean measured temperature distribution ranging from 86°C to 94.5°C.

The patterns of the measured temperature distribution show horizontally strip patterns. The original experimental image of Fig. 11 also show very similar patterns with those obtained by measurements though slight difference exists locally. The local difference between the original image and the calculation results is simply due to photographic expression. The original intensity data showed same distributions with calculated results, which implies that the constructed measurement system is capable of probing temperature field of thermal fluid.

Fig. 12 shows the measurement results under forced flow condition, unsteady condition. In this case, small amount of water was injected into the water tank from the bottom of the tank through a hole by opening a valve installed under the tank bottom. The jet water was injected maintaining the previous quiescent flow condition as shown on Fig. 12. It can be said that the forced thermal boundary layer is developing near the cartridge heater. The highest temperatures measured in the forced convection condition were 92.6 °C(left side) and

90.0°C(right side), respectively.

### 2.2 Velocity field measurements with a gray level cross correlation algorithm

For the measurement of velocity field, the gray-level cross-correlation method<sup>(17)</sup> was introduced. The color images captured were transformed into gray-level images for vector acquisition. Below Eq (6) was used for the calculation of the cross-correlation coefficients between two sets of gray-level images. The vector terminals were determined when these coefficients show the maximum value.

$$C_{fg} = \frac{\sum_{i=1}^{n^2} (f_i - \bar{f})(g_i - \bar{g})}{\sqrt{\sum_{i=1}^{n^2} (f_i - \bar{f})^2 \sum_{i=1}^{n^2} (g_i - \bar{g})^2}} \quad (6)$$

Here,  $f_i$  and  $g_i$  mean gray levels of the pixels within the correlation region and,  $\bar{f}$  and  $\bar{g}$  over these letters indicates the average value of the gray levels of the pixels within the correlation region. And  $n^2$  means the pixel number of the correlation area. Before calculating the coefficient, a pre-process, such as elimination of background image and noise reduction was carried out to get more accurate results. A post process was taken for more easy understanding for the obtained raw vector data. The background image was obtained by averaging about 120 the consecutive field images. The calculating time on the host computer(Pentium 1GHz) was about 1 minutes for the case that the grid for velocity vector extraction was set to 100 x 100, the

radius for the searching area was set to 20 pixels, the size for the correlation area was set to 32 x 32 pixels. Since there is an positional uncertainty with maximum  $\pm 1$  pixel when the terminal point of the velocity vector is obtained by the PIV based on pixel resolution, the sub-pixel interpolation method<sup>(17)</sup> was adopted for more accurate calculation. An error vector elimination method<sup>(20)</sup> based on the continuous flow condition was adopted.

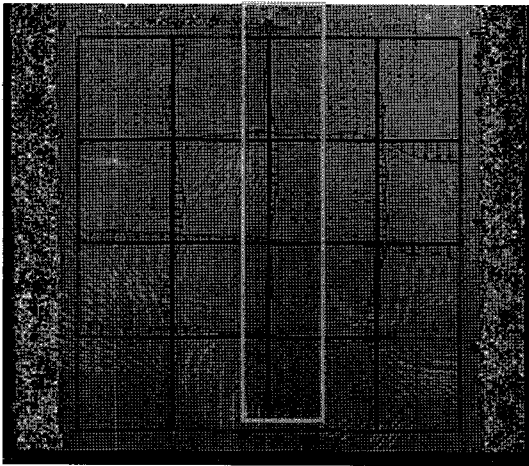


Fig. 13 Velocity field at  $t=t_0$

Fig. 13 shows one of the instantaneous velocity field obtained by the measurement system. This velocity field is obtained on the same image used for temperature measurement, which makes the constructed system possible simultaneous measurement for the two physical properties, temperature and velocity. It can be seen that there is a swirl-like vector field around the cartridge heater, which implies that the flow field shows a quite strong three-dimensionality. It is construed that the thermal flows play important roles to influence the

horizontal flows. Some physical features such as the convective turbulent heat transfer ( $T'u'$ ) and the radiations ( $\propto T^4$ ) over the whole field will be able to be estimated from the measured temperature and velocity fields, which is not attainable with any other measurement techniques like the hot wires or the cold wires.

### 3. Conclusions

Field-wise measurements for the thermal flows around a cartridge heater were successfully carried out. Measurements near the boiling point were successfully attained in the first. Measured temperature patterns for both natural and forced conditions showed good agreements with those of the original experimental image. This implies that the measurement system can quantify high temperature fields in water flows.

The velocity field was also successfully measured in simultaneous. The measured vector field around the cartridge heater indicated that a quite strong three-dimensional flow exists due to thermal plume occurred by strong heat flux from the heating body. It can be said that the thermal flows play important roles to influence the horizontal flows. Other physical properties such as the convective turbulent heat transfer and the radiations can be estimated quantitatively from the measured temperature and velocity fields, which could not obtainable with any other measurement techniques such as the hot wires or the cold wires. The

relative error for temperature field was about 5% over the measurable temperature range.

## References

- [1] Klein, E. J., 1968, Liquid Crystals for the Visualization of Unsteady Boundary Layers, *Third Canadian Congress of Applied Mechanics*, Calgary.
- [2] Lemberg, R., 1971, Liquid Crystals in Aerodynamic Testing, *Astronaut Aeronaut*, Vol. 6, pp.70-73.
- [3] McEldery, E. D., 1970, Boundary Layer Transitions on a Flat Plate, Air Force Flight Dynamics Lab., FDMG TM70-3.
- [4] Orden T. R. and Hendricks, E. W., 1984, Liquid Crystal Thermography in Water Tunnels, *Exp. in Fluids*, Vol. 2, pp.65-66.
- [5] Rhee, H. S. and Koseff, J.R., Flow Visualization of a Recirculation Flow by Rheoscopic Liquid Crystal Techiques, *Exp. in Fluids*, Vol. 12, pp.57-64.
- [6] Rhee, H. S., Koseff, J. R. and Street, R. L., 1986, Simultaneous Flow and Temperature Field Visualization in a Mixed Convection Flow, *Flow Visualization IV* (ed. Veret, C, Washington, Hemisphere), pp.659-664.
- [7] Dabiri, D. and Gharib, M., 1991, Digital Particle Image Thermometry: The Method Implementation, *Experiments in Fluids*, Vol. 11, pp.77-86.
- [8] Cooper, T. E., Field, R. J. and Meyer, J. F., 1975, Liquid Crystal Thermography and Its Application to the Study of Convective Heat Transfer, *J. Heat Transfer*, Vol.92, pp.422-450.
- [9] Wilcox, N. A., Watson, A.T. and Tatterson, G.B., 1985, Color/Temperature Calibrations for Temperature Sensitive Tracer Particles, *Proc. Intl. Symp. Physical and Numerical Flow Visualization*, Albuquerque, USA, pp.65-74.
- [10] Akino, M., Kunugi, T., Ichimiya, K., Mitsushiro, K. and Ueda, M., 1986, Improved Liquid-Crystal Thermometry Excluding Human Color Sensation: Concept and Calibration, *ASME FED*, Vol. 44, pp. 57-62.
- [11] Akino, N., Kungi, T., Ueda, M. and Kurosawa, A., 1988, Liquid-Crystal Thermometry Based on Automatic Color Evaluation and Applications to Measure Turbulent Heat Transfer, in *Transport Phenomena in Turbulent Flows*, pp.807-820.
- [12] Ozawa, M., Muller, U., Kimura, I. and Takamori, 1992, T., Flow and Temperature Measurement of Natural Convection in a Hele-Shaw Cell Using a Thermo-Sensitive Liquid-Crystal Tracer, *Exp. in Fluids*, Vol.12, pp.213-222.
- [13] Nozaki, T., Mochizuki, T., Kaji, N. and Mori, Y. H., 1995, Application of Liquid-Crystal Thermometry to Drop Temperature Measurements, *Exp. in Fluids*, Vol.18, pp.137-144.
- [14] Kimura, I., Kuroe, Y., Ozawa, M., 1993, Application of Neural Networks to Quantitative Flow Visualization, *J. Flow Visualization and Image Processing*, Vol. 1, pp.261-269.
- [15] Hwang, T. G., Doh, D. H., Kim, D.H., Bang, K. H., Moon, J. S.,

Hong, S.D., Chang, T. H., 2005, Improvements of Temperature Field Measurement Technique using Neural Network, KOSME, Vol. 29, No. 2, pp.209~216.

- [16] Chang, T. H. and Doh, D. H., 2003, An Experimental Study on Temperature and Velocity Fields of the Turbulent Flows Horizontal Cylindrical Tube by using Thermo-sensitive Liquid Crystal, Journal of Korean Society of Marine Engineers (KOSME), Vol.27, No.7, pp.921-929.
- [17] Utami T. and Blackwelder R., 1991, A cross correlation technique for velocity field extraction from particulate visualization, *Exp. in Fluids*, Vol. 10, pp.213-223.
- [18] Rumelhart, D. E., 1986, Parallel distributed processing, *The MIT Press*, Vol. 1.
- [19] ANSI/ASME MFC-2M, 1983, Measurement uncertainty for fluid flow in closed conduits.
- [20] Hojo K. and Takashima H., 1995, Detection of erroneous velocity vectors obtained in PIV, *J. of Visualization Society of Japan*, Vol. 15, Suppl. No.2, p.177.



### Tae-Gyu Hwang

He received a B.A (2001), M.Sc(2003) at KMU. He also received Ph.D degree at Dept. of Mech. Eng. at KMU(2005). His recent research areas are 3D PTV & 4D PIV applications (sphere wake, jet). His research interests are thermal flow visualization using 3D PIV, 3D PTV, 4D PTV and micro PIV techniques.



### Bon-Young Koo

He received a B.A (1987), M.Sc (1989) at Dong A Univ. He is a Ph.D candidate of Mech. Eng. at Pusan Nat'l Univ. since 2006. His major is refrigeration and air conditioning. His research interests are thermal flow visualization using 3D PIV, 3D PTV and micro PIV techniques. He works for LG Electronics since 1989 and he is in charge of development of refrigerator.



### Seok-Ro Kim

He received a B.A. (1986), M.Sc (1988) at Kyung Hee Univ. He is a Ph.D candidate of Mech. Eng. at Pusan Nat'l Univ. since 2005. He has been working for LG Electronics since 1989 at Eng. Design Dept., Refrigeration Division Digital Appliance Company. His major subjects are to develop refrigerator techniques such as refrigeration cycle, low noise and saving energy.

## Author Profile



### Deog-Hee Doh

He received a B.A.(1985) and M.Sc(1988) at Korea Maritime Univ.(KMU). He got Ph.D. degree at the Dept. of Mech. Eng. of the Univ. of Tokyo, Japan (1995). He developed a 3D PTV system. He worked for the AFERC(POSTECH) in 1995. He works for KMU at the Div. of Mech. and Info. Eng. Research areas are 3D PIV/PTVs, micro 4D PTVs for quantitative flow visualizations.